

RSC Advances



This is an *Accepted Manuscript*, which has been through the Royal Society of Chemistry peer review process and has been accepted for publication.

Accepted Manuscripts are published online shortly after acceptance, before technical editing, formatting and proof reading. Using this free service, authors can make their results available to the community, in citable form, before we publish the edited article. This *Accepted Manuscript* will be replaced by the edited, formatted and paginated article as soon as this is available.

You can find more information about *Accepted Manuscripts* in the [Information for Authors](#).

Please note that technical editing may introduce minor changes to the text and/or graphics, which may alter content. The journal's standard [Terms & Conditions](#) and the [Ethical guidelines](#) still apply. In no event shall the Royal Society of Chemistry be held responsible for any errors or omissions in this *Accepted Manuscript* or any consequences arising from the use of any information it contains.

Junfeng Wang,^a Weijun He,^{a,b} Xiaochu Qin,^c Xiaoyi Wei,^d Xinpeng Tian,^a Li Liao,^e Shengrong Liao,^a Bin Yang,^a Zhengchao Tu,^c Bo Chen,^e Fazuo Wang,^a Xiaojiang Zhou,^{b,*} and Yonghong Liu^{a,*}

^a CAS Key Laboratory of Tropical Marine Bio-resources and Ecology/Guangdong Key Laboratory of Marine Materia Medica/RNAM Center for Marine Microbiology, South China Sea Institute of Oceanology, Chinese Academy of Sciences, Guangzhou 510301, PR China;

^b College of Pharmacy, Hunan University of Chinese Medicine, Changsha 410208, PR China;

^c Guangzhou Institutes of Biomedicine and Health, Chinese Academy of Sciences, Guangzhou 510530, PR China;

^d Key Laboratory of Plant Resources Conservation and Sustainable Utilization, South China Botanical Garden, Chinese Academy of Sciences, Guangzhou 510650, China

^e SOA Key Laboratory for Polar Science, Polar Research Institute of China, Shanghai 200136, PR China;

* Author to whom correspondence should be addressed; E-Mail: yonghongliu@scsio.ac.cn; Tel./Fax:

(+86)-020-8902-3244; gale9888@163.com, Tel: +86-731-8845-8234.

Abstract: Three new indolyl diketopiperazine derivatives, penillines A and B (**1** and **3**), isopenilline A (**2**), together with seven known alkaloids compounds (*E*)-3-(1H-imidazole-4-ylmethylene)-6-(1H-indol-3-ylmethyl)-2,5-piperazinediol (**4**), penilloid A (**5**), meleagrins (**6**), neoxalins (**7**), questiomycin A (**8**), *N*-(2-hydroxyphenyl)-acetamide (**9**), 2-benzoxazolinone (**10**), were isolated from the Antarctic soil-derived fungus *Penicillium* sp. SCSIO 05705. The new structures of **1–3** were elucidated on the basis of 1D and 2D NMR, mass spectra, CD spectra, and quantum chemical calculation. All the isolated compounds were tested for their antiviral (H1N1 and H3N2), antituberculosis, antibacterial, and cytotoxic activities. Among them, compounds **6–8** had significant *in vitro* cytotoxicities against the K562, MCF-7, A549, U937, HeLa, DU145, HL60, and HT29 cell lines, with IC₅₀ values ranging from 2.73 to 17.7 μM. In addition, compound **8** showed potent antituberculosis activity with MIC value of 3.91 μM, and the inhibition effect was close to the positive control INH (isoniazid, MIC 2.04 μM). A possible biogenesis pathway for compounds (**1–7**) was proposed.

1. Introduction

2,5-diketopiperazines (DKPs) constitute an important class of densely functionalized structures characterized by the cyclic dipeptides from two α -amino acids, and exhibited a wide range of biological activities including anti-tumor, antifouling, antibiotic, anti-inflammatory, and immunoregulatory activities.¹⁻³ Among them, Plinabulin (NPI 2358) has entered phase-I and phase-II clinical studies for the treatment of non-small cell lung cancer, which was a fully synthetic analog of the natural product known as halimide from marine-derived *Aspergillus* sp. CNC-139.^{4,5} From in the late 1980s, more and more 2,5-DKPs were discovered from fungi and bacteria,⁶⁻¹⁰ and the complex and densely functionalized structures and the extraordinary range of biological activities of 2,5-DKPs have stimulated many total synthesis programmes.¹¹⁻¹⁵

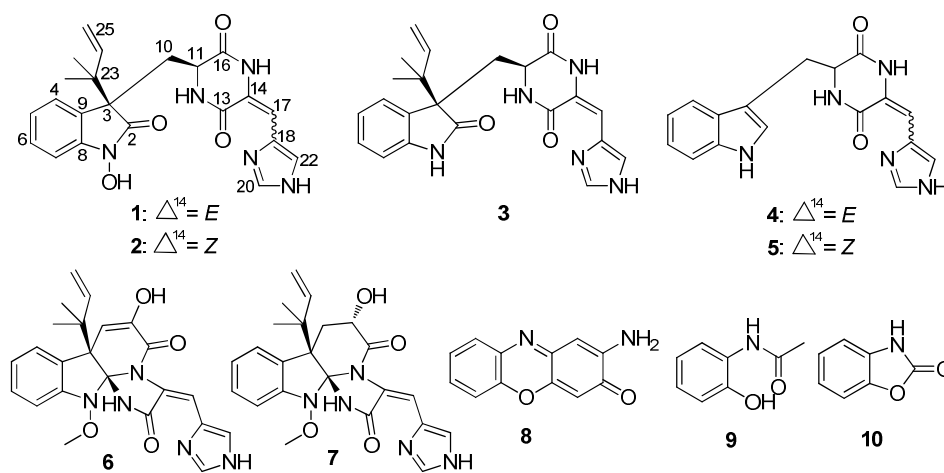


Fig. 1. The alkaloids **1–10** isolated from the Antarctic soil-derived fungus *Penicillium* sp. SCSIO 05705.

During our ongoing investigations from the fungal species inhabiting unique environments, a fungus, *Penicillium* sp. SCSIO 05705, obtained from a soil sample that was collected nearby the Great Wall station (Chinese Antarctic station, 62°12'59"S, 58°57'52"W), attracted our attention. The strain SCSIO 05705 was grown under static conditions at 24 °C for 40 days. The EtOAc extract of a fermentation broth of the fungus exhibited cytotoxic activity against the K562 and A549 cell lines at a concentration of 100 μ g/ml. Bioassay-guided fractionation of the bioactive

extract led to the isolation of three new indolyl diketopiperazine derivatives, penillines A and B (**1** and **3**), isopenilline A (**2**), together with seven known alkaloids compounds (*E*)-3-(1H-imidazole-4-ylmethylene)-6-(1H-indol-3-ylmethyl)-2,5-piperazinediol (**4**),¹⁶ peniloid A (**5**),¹⁶ meleagrins (**6**),¹⁷ neoxalins (**7**),¹⁴ questiomycin A (**8**),¹⁸ *N*-(2-hydroxyphenyl)-acetamide (**9**),¹⁹ 2-benzoxazolinone (**10**)²⁰ (Fig. 1). All the isolated compounds were evaluated for their antiviral (H1N1 and H3N2), antituberculosis, antibacterial, and cytotoxic activities. Herein, we report the isolation, structural elucidation and biological activities of these compounds.

2. Results and Discussion

2.1. Structural Elucidation

Compound (**1**) was obtained as yellow gum with the molecular formula C₂₂H₂₃N₅O₄ as determined by HRESIMS at *m/z* 420.1667 [M – H][–] (calcd 420.1667), indicating 14 degrees of unsaturation. Its ¹H NMR and ¹³C NMR (DEPT) spectra include signals for nine quaternary carbons (including three carbonyl carbons, four unsaturated carbons), eight unsaturated methine carbons, one saturated methine carbon, one unsaturated methylene carbon, one saturated methylene carbon, and two methyl carbons. The connectivity of the protons and C-atoms was established by the ¹H, ¹³C, HMQC spectrum (Table 1). The ¹H NMR spectrum showed characteristic signals for AA'BB' spin system [δ_{H} 7.19 (d, *J* = 7.5 Hz), 7.00 (t, *J* = 7.5 Hz), 7.24 (t, *J* = 7.5 Hz), and 6.89 (d, *J* = 7.5 Hz)], three olefinic protons of a terminal double bond [δ_{H} 6.00 (dd, *J* = 17.1, 10.8 Hz), δ_{H} 5.07 (d, *J* = 10.8 Hz), and δ_{H} 4.96 (d, *J* = 17.1 Hz)], three olefinic protons [δ_{H} 6.18 (s), 7.93 (s), 8.92 (s)], one methine (δ_{H} 3.49, m), one methylene [δ_{H} 2.53 (dd, *J* = 14.4, 2.9 Hz), and 2.39 (dd, *J* = 14.4, 7.6 Hz)], and two methyl groups [δ_{H} 0.91 (s), and 0.99 (s)]. The general features of its NMR spectroscopic data (Table 1) closely resembled those of roquefortine M.²¹ Detailed comparison of 1D and 2D NMR data of these two compounds suggested that they had the same structure. The cross-peaks between H-5 and

H-4/H-6, H-6 and H-5/H-7, H₂-10 and H-11, and H-24 and H₂-25 were observed in the ¹H-¹H COSY spectrum (Fig. 2). The key HMBC correlations of H₃-26 and H₃-27 with C-3 (δ_C 54.5) indicated that the isopentyl unit was directly connected to C-3 (Fig. 2). Besides, the double bond between C-14 and C-17 possessed the (*E*)-geometry, which was supported by key NOESY correlation between H-17 (δ_H 6.18, s) and 15-NH (δ_H 10.66, s). Additionally, the absolute configurations of **1** were determined as 3*R* and 11*S*, respectively, by comparing the calculated ECD spectrum with its experimental values (Fig. 3). Therefore, the structure of compound **1** (named penilline A) was proposed as roquefortine M, which had been previously obtained by natural product biosynthesis.²¹ To the best of our knowledge, this is the first report of penilline A (**1**) as a natural product. Due to the lack of corresponding data in the literature,²¹ the absolute configurations (3*R* and 11*S*) of **1** were also reported here for the first time.

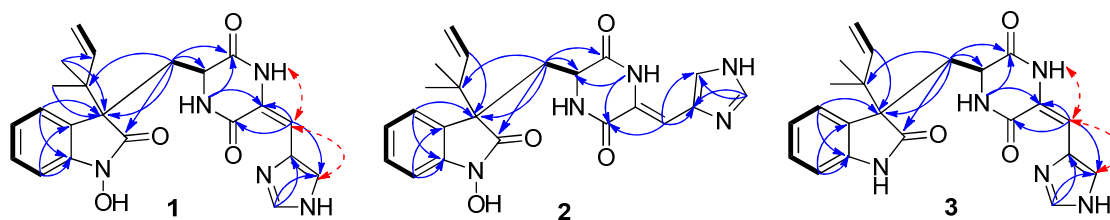


Fig. 2. The key ¹H-¹H COSY (bold), HMBC (arrows), and NOESY (dashed arrows) correlations of **1**–**3**.

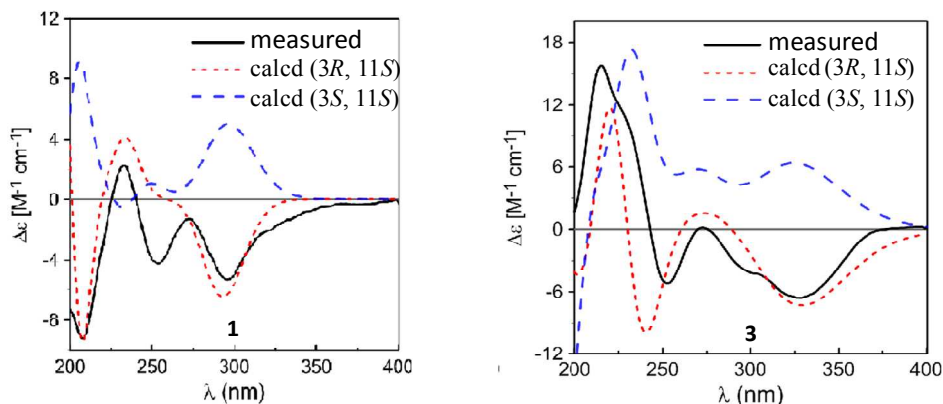


Fig. 3. Comparison between calculated (CAM-B3LYP/TZVP) and experimental ECD spectra of **1** and **3** in MeOH.

Compound (**2**) was obtained as yellow gum. It was assigned the same molecular formula $C_{22}H_{23}N_5O_4$ as **1** by HRESIMS (m/z 422.1811 $[M + H]^+$). Its 1D NMR spectra showed resonances nearly identical with those of **1**. These results suggested the same planar structure for the two metabolites. According to the double bond between (*E*)-3-(1H-imidazole-4-ylmethylene)-6-(1H-indol-3-ylmethyl)-2,5-piperazinediol (**4**) and penilloid A (**5**),¹⁶ the (*Z*)-geometry of the double bond between C-14 and C-17 in **2** was established by comparison of its spectral properties with those of its geometric isomer **1** that has the (*E*)-geometry. The chemical shifts of H-17 (δ_H 6.18, s), H-20 (δ_H 8.92, s), and H-22 (δ_H 7.93, s) in **1** were changed dramatically to H-17 (δ_H 6.46, s), H-20 (δ_H 7.89, s), and H-22 (δ_H 7.45, s) in **2**. In addition, the chemical shift of C-18 was shifted from δ_C 127.0 in **1** to δ_C 136.3 in **2**. This variation indicated H-17 in **2** was shielded by being close to the carbonyl group (C-13), which was consistent with those of (*E*)-3-(1H-imidazole-4-ylmethylene)-6-(1H-indol-3-ylmethyl)-2,5-piperazinediol (**4**) and penilloid A (**5**).¹⁶ Further evidence for 14*Z* configuration of **2** was given by the maximum UV absorption band at 313 nm, comparable to that of 323 nm in **1**.²² The similarity of CD curve [CD (*c* 0.02, MeOH) ($\Delta\epsilon_{max}$) 205 (−9.78), 232 (+4.89), 249 (−6.22), 271 (+0.78), 292 (−6.34)] of **2** with those of **1** [CD (*c* 0.02, MeOH) ($\Delta\epsilon_{max}$) 208 (−14.22), 233 (+3.51), 252 (−6.52), 272 (−2.00), 295 (−8.27)] indicated the same configurations of chiral carbons between **2** and **1** (Fig. S1).

Compound (**3**) was obtained as a colorless gum with the molecular formula $C_{22}H_{23}N_5O_3$ assigned from HRESIMS data with one oxygen atom less than **1** and **2**. The UV spectrum displayed absorption bands at 209 and 326 nm, consistent with those of **1**. The 1H and ^{13}C NMR data of **3** were almost the same as those of compound **1**. However, the indolyl moiety of compound **3** did not match with data for that of compound **1**. The ^{13}C NMR chemical shifts for C-2 differed significantly (**3** δ_C 179.2; **1** δ_C 172.4), supporting the absence of an *N*-hydroxy

group in **3**. The key COSY and HMBC correlations of **3** were in good agreement with the data for **1**. Furthermore, the double bond between C-14 and C-17 also possessed the (*E*)-geometry, which was supported by key NOESY correlation between H-17 (δ_{H} 5.73, s) and 15-NH (δ_{H} 10.17, s) in DMSO-*d*₆. The absolute configurations of **3** were further determined as 3*R* and 11*S*, respectively, by comparing the calculated ECD curve with its experimental values, consistent with the corresponding absolute configurations in compound **1** (Fig. 3). Therefore, the structure of **3** was proposed and named penilline B.

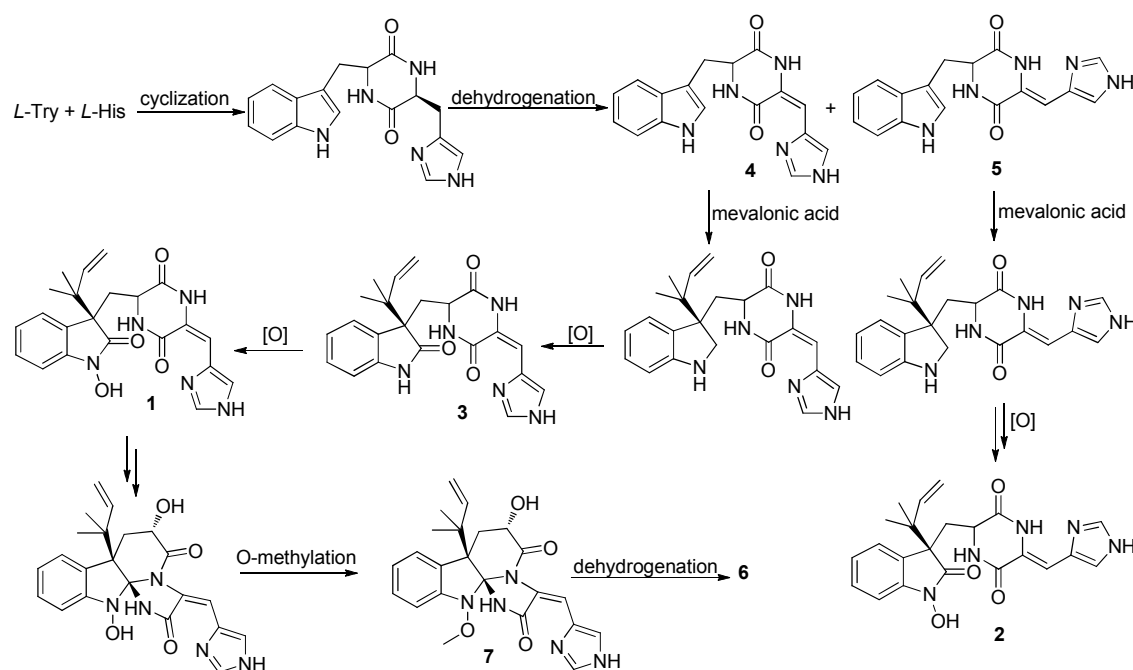
Table 1. ¹H and ¹³C NMR Data for **1–3** (500, 125 MHz, DMSO-*d*₆, TMS, δ ppm).

No.	1		2		3	
	δ_{C}	δ_{H} (<i>J</i> in Hz)	δ_{C}	δ_{H} (<i>J</i> in Hz)	δ_{C}	δ_{H} (<i>J</i> in Hz)
2	172.4, C		172.7, C		179.2, C	
3	54.5, C		55.0, C		54.9, C	
4	125.5, CH	7.19, d (7.5)	125.2, CH	7.19, d (7.7)	127.2, CH	7.03, d (7.7)
5	121.7, CH	7.00, t (7.5)	121.7, CH	7.02, t (7.6)	121.2, CH	6.86, t (7.5)
6	128.5, CH	7.24, t (7.5)	128.5, CH	7.29, t (7.6)	128.3, CH	6.98, t (7.5)
7	107.0, CH	6.89, d (7.5)	107.0, CH	6.96, d (7.7)	108.7, CH	6.43, d (7.7)
8	143.3, C		143.6, C		143.4, C	
9	124.9, C		124.2, C		126.9, C	
10	35.2, CH ₂	2.53, dd (14.4, 2.9); 2.39, dd (14.4, 7.6)	36.4, CH ₂	2.63, dd (14.3, 7.2); 2.32, d (14.3)	33.8, CH ₂	2.55, d (14.5); 2.45, dd (14.9, 7.6)
11	52.7, CH	3.49, m	52.6, CH	3.29, d (7.2)	53.2, CH	3.94, d (7.6)
12		7.93, brs		*		8.26, brs
13	159.5, C		158.6, C		158.5, C	
14	128.0, C		*		126.9, C	
15		10.66, brs		11.39, brs		10.17, brs
16	165.7, C		164.5, C		165.8, C	
17	103.6, CH	6.18, s	104.0, CH	6.46, s	102.9, CH	5.73, s
18	127.0, C		136.3, C		127.1, C	
20	134.1, CH	8.92, s	136.4, CH	7.89, s	133.9, CH	8.88, s
22	121.1, CH	7.93, s	118.9, CH	7.45, s	121.2, CH	7.86, s
23	42.4, C		42.1, C		42.1, C	
24	142.7, CH	6.00, dd (17.1, 10.8)	142.8, CH	6.01, dd (17.4, 10.9)	143.0, CH	5.96, dd (17.4, 10.8)
25	114.3, CH ₂	5.07, d (10.8); 4.96, d (17.1)	114.2, CH ₂	5.08, d (10.9); 4.97, d (17.4)	113.7, CH ₂	5.05, d (10.8); 4.93, d (17.4)
26	21.9, CH ₃	0.99, s	21.9, CH ₃	1.02, s	21.5, CH ₃	0.99, s
27	21.5, CH ₃	0.91, s	21.6, CH ₃	0.93, s	21.1, CH ₃	0.87, s

* Not observed.

2.2. The Postulated Biogenesis Pathway of Compounds 1–7

To the best of our knowledge, roquefortines are the very complex alkaloids in nature, which are produced by fungus. They are derived from histidine and tryptophan. Most of them are substituted by isopentenyl at the C-3 of indole, and imidazole is connected with the diketopiperazine ring by single or double bond. In the plausible biogenesis of 1–7, compounds 4 and 5 could be the plausible biosynthetic precursors for 1–3, 6 and 7. This pathway involves cyclisation, dehydrogenation, oxidation, ring opening/closure, and methylation to form compounds (1–7) (Scheme 1).



Scheme 1. The postulated biogenesis pathway of 1–7.

2.3. Biological Activities

All the isolated compounds (1–10) were evaluated for their antiviral (H1N1 and H3N2), cytotoxic (the K562, MCF-7, A549, U937, HeLa, DU145, HL60, and HT29 cell lines), antibacterial (*Escherichia coli* and *Staphylococcus aureus*), and antituberculosis activities. Among them, compounds 6–8 had significant *in vitro* cytotoxicities against the K562, MCF-7, A549, U937, HeLa, DU145, HL60, and HT29 cell lines, with IC₅₀ values ranging from 2.73 to

17.7 μM (Table 2). In addition, compound **8** showed potent antituberculosis activity with MIC value of 3.91 μM , and the inhibition effect was close to the positive control INH (isoniazid, MIC 2.04 μM), whereas none of the compounds exhibited antiviral activities against H1N1 and H3N2 influenza viruses or any additional antibacterial activities (MIC > 100 μM).

Table 2. Cytotoxicities against tumor cells for **6–8**.

Cell lines ^a	IC ₅₀ (μM)			
	6	7	8	Taxol (nM) ^b
K562	3.56 \pm 0.48	3.97 \pm 0.30	7.64 \pm 0.93	7.17 \pm 0.14
MCF-7	12.8 \pm 0.78	11.7 \pm 0.70	7.06 \pm 0.10	7.32 \pm 0.23
A549	5.47 \pm 0.35	6.39 \pm 0.34	12.9 \pm 0.92	2.12 \pm 0.06
U937	2.73 \pm 0.51	4.91 \pm 0.33	17.5 \pm 1.88	1.66 \pm 0.08
Hela	4.16 \pm 0.21	5.79 \pm 0.20	17.7 \pm 1.48	3.01 \pm 0.11
DU145	6.75 \pm 0.36	8.84 \pm 0.75	14.9 \pm 1.69	2.30 \pm 0.04
HL60	3.70 \pm 0.20	5.29 \pm 0.21	NT ^c	1.99 \pm 0.03
HT29	5.57 \pm 0.44	9.00 \pm 0.09	16.7 \pm 1.75	3.04 \pm 0.04

^a Each value represents mean \pm SD of three experiments.

^b Taxol was used as positive control.

^c NT = not tested.

3. Experimental Section

3.1. General Experimental Procedures

Optical rotations were measured with a PerkinElmer 341 polarimeter. UV spectra were recorded on a Shimadzu UV-2401PC spectrometer. Circular dichroism spectra were recorded with a Chirascan circular dichroism spectrometer (Applied Photophysics, Ltd). ¹H, ¹³C NMR, DEPT, and 2D-NMR spectra were recorded on the Bruker DRX-500 spectrometer using TMS as internal standard and chemical shifts were recorded as δ -values. HRESIMS (including ESIMS) spectra were recorded on an Applied Biosystems Mariner 5140 spectrometer. TLC and column chromatography (CC) were performed on plates precoated with silica gel GF₂₅₄ (10–40 μm) and over silica gel (200–300 mesh) (Qingdao Marine Chemical Factory, China), and Sephadex LH-20 (Amersham Biosciences, Sweden), respectively. All solvents used were of analytical

grade (Tianjin Fuyu Chemical and Industry Factory). Semipreparative HPLC was performed using an ODS column (YMC-pack ODS-A, 10 × 250 mm, 5 μm, 4 mL/min).

3.2. Fungal Materials

The fungal strain, *Penicillium* sp. SCSIO 05705, was isolated from a soil sample that was collected nearby the Great Wall station (Chinese Antarctic station, 62°12'59"S, 58°57'52"W), and identified by associate professor Xinpeng Tian, one of our authors. It was identified according to its morphological characteristics and ITS gene sequences (GenBank Accession No. KR824116). A reference culture is deposited in at our laboratory at -80 °C. The producing strain was prepared on potato dextrose agar slants at 3.3% salt concentration and stored at 4 °C.

3.3. Fermentation and Extraction

Penicillium sp. SCSIO 05705 was grown under static conditions at 24 °C for 40 days in one hundred 1000 mL conical flasks containing liquid medium (300 mL/flask) composed of mannitol (20 g/L), maltose (20 g/L), glucose (10 g/L), monosodium glutamate (10 g/L), KH₂PO₄ (0.5 g/L), MgSO₄ (0.3 g/L), and yeast extract (3 g/L), and tap water after adjusting its pH to 7.5. The fermented whole broth (30 L) was filtered through cheesecloth to separate it into filtrate and mycelia. The filtrate was concentrated under vacuum to about a quarter of original volume and then extracted three times with EtOAc to give an EtOAc solution, while the mycelia were extracted three times with acetone. The acetone solution was evaporated under reduced pressure to afford an aqueous solution. The aqueous solution was extracted three times with EtOAc to give another EtOAc solution. Both EtOAc solutions were combined and concentrated under reduced pressure to give a dark brown gum (12.9 g).

3.4. Purification

The EtOAc extract (12.9 g) was subjected to vacuum liquid chromatography (VLC) on a silica gel column using step gradient elution with MeOH-CH₂Cl₂ (0-100%) to separate into nine

fractions based on TLC properties. Fraction 2 (1.1 g) was further separated into four subfractions by Sephadex LH-20 eluting with MeOH-CH₂Cl₂ (1:1). Subfraction 2-2 (84 mg) was purified by semipreparative HPLC (20% CH₃CN-H₂O) to yield **9** (3.8 mg, *t_R* 10.1 min). Subfraction 2-3 (127 mg) was purified by semipreparative HPLC (25% CH₃CN-H₂O) to yield **10** (12.6 mg, *t_R* 10.8 min) and **8** (3.6 mg, *t_R* 22.9 min), respectively. Fraction 3 (670 mg) was separated into four subfractions by Sephadex LH-20 eluting with MeOH. Subfraction 3-2 (260 mg) was additionally separated by semipreparative HPLC (25% CH₃CN-H₂O) to yield **6** (73.0 mg, *t_R* 28.1 min). Subfraction 3-3 (145 mg) was separated by semipreparative HPLC (40% CH₃CN-H₂O) to yield **7** (20.0 mg, *t_R* 18.4 min). Fraction 4 (530 g) was further separated into five subfractions by reverse phase silica gel (ODS) using step gradient elution with MeOH-H₂O (20%–100%). Subfraction 4-1 (92 mg) was further separated by semipreparative HPLC (30% CH₃CN-H₂O) to yield **2** (10.7 mg, *t_R* 22.7 min). Subfraction 4-3 (78 mg) was separated by semipreparative HPLC (20% CH₃CN-H₂O) to yield **5** (15.7 mg, *t_R* 19.2 min). Fraction 5 (870 mg) was further separated into four subfractions by Sephadex LH-20 eluting with MeOH. Subfraction 5-3 (325 mg) was additionally separated by semipreparative HPLC (23% CH₃CN-H₂O) to **4** (17.2 mg, *t_R* 6.6 min), **3** (9.1 mg, *t_R* 18.1 min), and **1** (46.4 mg, *t_R* 21.2 min).

Penilline A (**1**): yellow gum; $[\alpha]_D^{25} -125.6$ (*c* 4.6, CH₃OH); UV (MeOH) λ_{\max} (log ϵ): 209 (4.18), 326 (3.97) nm; CD (*c* 0.02, MeOH) ($\Delta\epsilon_{\max}$): 208 (−14.22), 233 (+3.51), 252 (−6.52), 272 (−2.00), 295 (−8.27); ¹H NMR and ¹³C NMR data, see Table 1; HRESIMS *m/z* 420.1667 [M − H][−] (calcd for C₂₂H₂₂N₅O₄, 420.1667).

Isopenilline A (**2**): yellow gum; $[\alpha]_D^{25} -57.9$ (*c* 1.1, CH₃OH); UV (MeOH) λ_{\max} (log ϵ): 210 (4.34), 313 (4.18) nm; CD (*c* 0.02, MeOH) ($\Delta\epsilon_{\max}$): 205 (−9.78), 232 (+4.89), 249 (−6.22), 271 (+0.78), 292 (−6.34); ¹H NMR and ¹³C NMR data, see Table 1; HRESIMS *m/z* 422.1811 [M + H]⁺ (calcd for C₂₂H₂₄N₅O₄, 422.1823).

Penilline B (**3**): yellow gum; $[\alpha]_D^{25} -149.7$ (c 0.9, CH₃OH); UV (MeOH) λ_{\max} ($\log \epsilon$): 209 (4.16), 326 (3.95) nm; CD (c 0.02, MeOH) ($\Delta\epsilon_{\max}$): 215 (+26.11), 252 (-8.22), 329 (-11.05); ¹H NMR and ¹³C NMR data, see Table 1; HRESIMS m/z 406.1863 [M + H]⁺ (calcd for C₂₂H₂₄N₅O₃, 406.1874).

3.5. Computational Details

Molecular Merck force field (MMFF) and DFT/TDDFT calculations were performed with Spartan'14 software package (Wavefunction Inc., Irvine, CA, USA) and Gaussian09 program package,²³ respectively, using default grids and convergence criteria. MMFF conformational search generated low-energy conformers within a 10 kcal/mol energy window were subjected to geometry optimization using DFT method at the B3LYP/6-31G (d) level. Frequency calculations were run at the same level to verify that each optimized conformer was a true minimum and to estimate their relative thermal free energies (ΔG) at 298.15K. Energies of the low-energy conformers in MeOH were re-calculated at the B3LYP/def2-TZVP level. Solvent effects were taken into account by using polarizable continuum model (PCM). The TDDFT calculations were performed using the hybrid B3LYP and CAM-B3LYP functionals, and the Ahlrichs' basis set TZVP (triple zeta valence plus polarization).²⁴ The number of excited states was 40 for all compounds. The CD spectra were generated by the program SpecDis²⁵ using a Gaussian band shape with 0.28 or 0.30 eV exponential half-width from dipole-length dipolar and rotational strengths. The equilibrium population of each conformer at 298.15K was calculated from its relative free energies using Boltzmann statistics. The calculated spectra were generated from the low-energy conformers according to the Boltzmann weighting of each conformer in MeOH solution.

3.6. Bioassay Protocols

Cytotoxicity was assayed with the CCK-8 (Dojindo, Japan) method.²⁶ Cell lines, K562,

MCF-7, A549, U937, HeLa, DU145, HL60, and HT29 were purchased from Shanghai Cell Bank, Chinese Academy of Sciences. Cells were routinely grown and maintained in mediums RPMI or DMEM with 10% FBS and with 1% penicillin/streptomycin. All cell lines were incubated in a Thermo/Forma Scientific CO₂ Water Jacketed Incubator with 5% CO₂ in air at 37 °C. Cell viability assay was determined by the CCK-8 (Dojindo, Japan) assay. Cells were seeded at a density of 400-800 cells/well in 384 well plates and treated with various concentration of compounds or solvent control. After 72 h incubation, CCK-8 reagent was added, and absorbance was measured at 450 nm using Envision 2104 multi-label Reader (Perkin Elmer, USA). Dose response curves were plotted to determine the IC₅₀ values using Prism 5.0 (GraphPad Software Inc., USA). Taxol was used as the positive control with IC₅₀ values of 7.17, 7.32, 2.12, 1.66, 3.01, 2.30, 1.99, and 3.04 nM, respectively.

The H37Ra strain of *M. tuberculosis* was used for the anti-TB bioassay.²⁷ The test materials were dissolved in DMSO at 10 mg/mL and tested in a series of 2-fold dilutions with the highest concentration of 100 µg/mL (and 1% v/v DMSO). Samples were incubated for 7 days with *M. tuberculosis* in a 96-well plates, and then cell growth was determined using the Alamar Blue dye with fluorometric detection. The MIC was defined as the lowest concentration resulting in ninety percent or greater inhibition of fluorescence compared to bacteria-only controls. INH (isoniazid) was used as the positive control with MIC value of 2.04 µM.

The antiviral activities against H1N1 and H3N2 were evaluated by the CPE inhibition assay.²⁸ Confluent MDCK cell monolayers were firstly incubated with influenza virus at 37 °C for 1 h. After removing the virus dilution, cells were maintained in infecting media (RPMI 1640, 4 µg/mL of trypsin) containing different concentrations of test compounds. After 48 h incubation at 37 °C, the cells were fixed with 100 µL of 4% formaldehyde for 20 min at room temperature. After removal of the formaldehyde, the cells were stained with 0.1% crystal violet for 30 min.

The plates were washed and dried, and the intensity of crystal violet staining for each well was measured in a microplate reader (Bio-Rad, Hercules, CA, USA) at 570 nm. The IC₅₀ was calculated as the compound concentration required inhibiting influenza virus yield at 48 h post-infection by 50%. Tamiflu was used as the positive control with IC₅₀ values of 16.9 and 18.5 nM, respectively.

The antimicrobial activities against *Staphylococcus aureus*, and *Escherichia coli* were evaluated by an agar dilution method.²⁹ The tested strains were cultivated in LB agar plates for bacteria at 37 °C. Compounds and positive control were dissolved in DMSO at different concentrations from 100 to 0.05 µg/mL by the continuous 2-fold dilution methods. A 5 µL quantity of test solution was absorbed by a paper disk (5 mm diameter) and placed on the assay plates. After 24 h incubation, zones of inhibition (mm in diameter) were recorded. The minimum inhibitory concentrations (MICs) were defined as the lowest concentration at which no microbial growth could be observed. Ciprofloxacin lactate was used as positive control for *S. aureus* and *E. coli* with MIC values of 3.78 and 0.06 µM, respectively.

4. Conclusions

The investigation aimed at exploring structurally novel and bioactive secondary metabolites from fungal species inhabiting unique environments, a fungus, *Penicillium* sp. SCSIO 05705, obtained from a soil sample that was collected nearby the Great Wall station (Chinese Antarctic station, 62°12'59"S, 58°57'52"W), was selected for chemical study because its secondary metabolites exhibited cytotoxic activity against the K562 and A549 cell lines at a concentration of 100 µg/ml. Bioassay-guided fractionation of the bioactive extract led to the isolation of three new indolyl diketopiperazine derivatives, penillines A and B (**1** and **3**), isopenilline A (**2**), together with seven known alkaloids compounds (*E*)-3-(1H-imidazole-4-ylmethylene)-6-(1H-indol-3-ylmethyl)-2,5-piperazinediol (**4**), penilloid A (**5**), meleagrins (**6**), neoxalines (**7**), questionmycins (**8**), *N*-(2-hydroxyphenyl)-acetamide (**9**),

2-benzoxazolinone (**10**). All the isolated compounds were tested for their antiviral (H1N1 and H3N2), antituberculosis, antibacterial, and cytotoxic activities. Among them, compounds **6–8** had significant *in vitro* cytotoxicities against the K562, MCF-7, A549, U937, Hela, DU145, HL60, and HT29 cell lines, with IC₅₀ values ranging from 2.73 to 17.7 μM. In addition, compound **8** showed potent antituberculosis activity with MIC value of 3.91 μM, and the inhibition effect was close to the positive control INH (isoniazid, MIC 2.04 μM).

Acknowledgments

This work was financially supported by the National Key Basic Research Program of China (973)'s Project (2011CB915503), the Open Foundation of the SOA key Laboratory for Polar Science, Polar Research Institute of China (KP201305), the National High Technology Research and Development Program (863 Program, 2012AA092104), the National Natural Science Foundation of China (Nos. 31270402, 21172230, 41476135, and 41476136), the Strategic Priority Research Program of the Chinese Academy of Sciences (XDA11030403), Guangdong Marine Economic Development and Innovation of Regional Demonstration Project (GD2012-D01-001).

Conflicts of Interest

The authors declare no conflict of interest.

References and Notes

1. A. D. Borthwick, *Chem Rev*, 2012, **112**, 3641–3716.
2. Y. Wang, P. Wang, H. G. Ma, W. M. Zhu, *Expert Opin Ther Patents*, 2013, **23**, 1–19.
3. J. H. Chen, X. P. Lan, Y. H. Liu, A. Q. Jia, *Bioorg Med Chem Lett*, 2012, **22**, 3177–3180.
4. A. M. S. Mayer, K. B. Glaser, C. Cuevas, R. S. Jacobs, W. Kem, R. D. Little, J. M.

- McIntosh, D. J. Newman, B. C. Potts, D. E. Shuster, *Trends Pharmacol Sci*, 2010, **31**, 255–265.
5. W. H. Gerwick, B. S. Moore, *Chem Biol*, 2012, **19**, 85–98.
 6. F. D. Kong, Y. Wang, P. P. Liu, T. H. Dong, W. M. Zhu, *J Nat Prod*, 2014, **77**, 132–137.
 7. L. H. Meng, P. Zhang, X. M. Li, B. G. Wang, *Mar Drugs*, 2015, **13**, 276–287.
 8. J. F. Wang, Z. Y. Lu, P. P. Liu, Y. Wang, J. Li, K. Hong, W. M. Zhu, *Planta Med*, 2012, **78**, 1861–1866.
 9. P. Wang, L. J. Xi, P. P. Liu, Y. Wang, W. Wang, Y. Huang, W. M. Zhu, *Mar Drugs*, 2013, **11**, 1035–1049.
 10. X. W. Yang, G. Y. Zhang, J. X. Ying, B. Yang, X. F. Zhou, A. Steinmetz, Y. H. Liu, N. Wang, *Mar Drugs*, 2013, **11**, 33–39.
 11. L. Zhao, J. P. May, J. Huang, D. M. Perrin, *Org Lett*, 2012, **14**, 90–93.
 12. J. M. Roe, R. A. B. Webster, A. Ganesan, *Org Lett*, 2003, **5**, 2825–2827.
 13. J. M. Schkeryantz, J. C. G. Woo, P. Siliphaivanh, K. M. Depew, S. J. Danishefsky, *J Am Chem Soc*, 1999, **121**, 11964–11975.
 14. T. Ideguchi, T. Yamada, T. Shirahata, T. Hirose, A. Sugawara, Y. Kobayashi, S. Omura, T. Sunazuka, *J Am Chem Soc*, 2013, **135**, 12568–12571.
 15. S. R. Liao, Y. Xu, Y. Tang, J. F. Wang, X. F. Zhou, L. Xu, Y. H. Liu, *RSC Adv*, 2015, **5**, 51020–51026.
 16. F. He, Z. Han, J. Peng, P. Y. Qian, S. H. Qi, *Nat Prod Comm*, 2013, **8**, 329–332.
 17. K. I. Kawai, K. Nozawa, S. Nakajima, Y. Iitaka, *Chem Pharm Bull*, 1984, **32**, 94–98.
 18. Y. Igarashi, K. Takagi, T. Kajiura, T. Furumai, T. Oki, *J Antibiot*, 1998, **51**, 915–920.
 19. K. Pusecker, H. Laatsch, E. Heimke, H. Weyland, *J Antibiot*, 1997, **50**, 479–483.
 20. L. J. Zhong, M. Y. Huang, J. G. Zhang, G. W. Li, Y. H. Zhang, *Chin J Mar Drugs*, 2012,

- 31, 23–28.
21. M. I. Ries, H. Ali, P. P. Lankhorst, T. Hankemeier, R. A. Bovenberg, A. J. M. Driessen, R. J. Vreeken, *J Biol Chem*, 2013, **288**, 37289–37295.
22. P. M. Scott, J. Polonsky, M. A. Merrien, *J Agric Food Chem*, 1979, **27**, 201–202.
23. M. J. Frisch, G. W. Trucks, H. B. Schlegel, G. E. Scuseria, M. A. Robb, J. R. Cheeseman, G. Scalmani, V. Barone, B. Mennucci, G. A. Petersson, H. Nakatsuji, M. Caricato, X. Li, H. P. Hratchian, A. F. Izmaylov, J. Bloino, G. Zheng, J. L. Sonnenberg, M. Hada, M. Ehara, K. Toyota, R. Fukuda, J. Hasegawa, M. Ishida, T. Nakajima, Y. Honda, O. Kitao, H. Nakai, T. Vreven, J. A. Montgomery, J. E. Peralta, F. Ogliaro, M. Bearpark, J. J. Heyd, E. Brothers, K. N. Kudin, V. N. Staroverov, T. Keith, R. Kobayashi, J. Normand, K. Raghavachari, A. Rendell, J. C. Burant, S. S. Iyengar, J. Tomasi, M. Cossi, N. Rega, J. M. Millam, M. Klene, J. E. Knox, J. B. Cross, V. Bakken, C. Adamo, J. Jaramillo, R. Gomperts, R. E. Stratmann, O. Yazyev, A. J. Austin, R. Cammi, C. Pomelli, J. W. Ochterski, R. L. Martin, K. Morokuma, V. G. Zakrzewski, G. A. Voth, P. Salvador, J. J. Dannenberg, S. Dapprich, A. D. Daniels, O. Farkas, J. B. Foresman, J. V. Ortiz, J. Cioslowski, D. J. Fox, Gaussian 09, revision C.01. Gaussian, Inc.: Wallingford CT, **2010**.
24. A. Schäfer, C. Huber, R. Ahlrichs, *J. Chem. Phys.* 1994, **100**, 5829–5835.
25. T. Bruhn, A. Schaumlöffel, Y. Hemberger, G. Bringmann, *Chirality* 2013, **25**, 243–249
26. J. F. Wang, X. Y. Wei, X. C. Qin, X. P. Lin, X. F. Zhou, S. R. Liao, B. Yang, J. Liu, Z. C. Tu, Y. H. Liu, *Org Lett*, 2015, **17**, 656–659.
27. J. F. Wang, Z. Wang, Z. R. Ju, J. T. Wan, S. R. Liao, X. P. Lin, T. Y. Zhang, X. F. Zhou, H. Chen, Z. C. Tu, Y. H. Liu, *Planta Med*, 2015, **81**, 160–166.
28. W. Fang, X. P. Lin, X. F. Zhou, J. T. Wan, X. Lu, B. Yang, W. Ai, J. Lin, T. Y. Zhang, Z. C. Tu, Y. H. Liu, *Med Chem Commun*, 2014, **5**, 701–705.
29. J. F. Wang, X. P. Lin, C. Qin, S. R. Liao, J. T. Wan, T. Y. Zhang, J. Liu, M. Fredimoses, H. Chen, B. Yang, X. F. Zhou, X. W. Yang, Z. C. Tu, Y. H. Liu, *J Antibiot*, 2014, **67**, 581–583.